High-power, high-energy Ho:YAG oscillator pumped by a Tm-doped fiber laser

Encai Ji (吉恩才), Qiang Liu (柳 强)*, Zhenyue Hu (胡震岳), Ping Yan (闫 平), and Mali Gong (巩马理)

Department of Precision Instrument, State Key Laboratory of Precision Measurement Technology and Instruments, Center for Photonics and Electronics, Tsinghua University, Beijing 100084, China

**Corresponding author: qiangliu@mail.tsinghua.edu.cn*

Received August 11, 2015; accepted October 27, 2015; posted online December 7, 2015

A high-power, high-energy Ho:YAG oscillator resonantly pumped by a Tm-doped fiber laser is presented. A maximum continuous output power of 38 W with a slope efficiency of 51.9% is achieved at the wavelength of 2.09 μm, and $M^2 \approx 1.48$. In the *Q*-switching regime, the maximum pulse energy of 12.8 mJ, corresponding to a 514.5 kW peak power, is obtained at the pulse repetition frequency of 1 kHz. Furthermore, the thermal lens effect of the system is studied theoretically, and the radius of the transverse electromagnetic (TEM_{00}) mode of the laser crystal under different pump powers is given.

OCIS codes: 140.3540, 140.3580, 140.5680.

doi: 10.3788/COL201513.121402.

Lasers operating on the 2 μm wavelength range, due to the low attenuation in the atmosphere and their "eye-safety" aspects, are extremely useful for a variety of scientific and technical applications, such as lidar systems, spectroscopy, range finders, countermeasures, and the non-linear optical generation of mid-infrared radiation[1–3]. At present, 2 μm lasers based on thulium (Tm^{3+}) and holmium (Ho^{3+}) have attracted great interest in recent years. They are the best choice to get to the shorter wavelength region (1.85–2.05 μm) for Tm^{3+}-doped lasers operating on the ${}^3F_4 \rightarrow {}^3H_6$ transitions pumped directly into ${}^3H_4$ level by laser diodes (LDs) at 790 nm[4]. However, for longer ($\lambda > 2.05$ μm) wavelengths, lasing on ${}^5I_7 \rightarrow {}^5I_8$ transitions in Ho^{3+}-doped media is required. YAG, YALO, YVO4, LLF, YLF, BYF, and Lu_2O_3 crystals are all efficient laser hosts for 2 μm generation[5–8]. Additionally, YAG- and LuAG-based transparent ceramics are also competitive with their corresponding single crystals[9,10]. In general, the Ho:YAG crystal is more attractive for a high-power or high-energy laser due to its large thermal conductivity, hardness, reliable optical quality, and low cost. Recently, high-power 1.9 μm LDs were developed rapidly, and applied successfully in pumping various holmium crystals[8,11,12]. However, the low spectral brightness and bad beam quality have affected their applications, especially for developing high-power holmium lasers. So, high-power 1.9 μm lasers are mostly built with Tm^{3+}-doped gain elements. Although co-doping with Tm^{3+} is a feasible solution[13,14], it leads to very strong cooperative upconversion losses and hence a significant reduction in the effective upper level lifetime and increased thermal loading[15]. A Ho^{3+}-doped crystal resonantly pumped by a 1.91 μm Tm^{3+} laser can solve the above difficulties. Recently, high-power Tm-doped fiber lasers (TDFLs) have been widely used as the pump source, mostly because they can distribute the thermal load over a much larger length than the bulk Tm lasers, thus making heat removal less critical.

For 2.1 μm continuous wave (CW) Ho:YAG lasers pumped by TDFLs, in 2010, Mu *et al.*[16] reported 18.6 W of output power with an optical-to-optical efficiency of 78.5%. The system has much lower output power but higher efficiency compared with the 111 W Ho:YAG laser system pumped by a Tm:YLF laser[17] and the 55 W Ho:YAG laser system pumped by a GaSb diode stack[18] that was used in 2012. As for 2.1 μm pulsed holmium laser pumped by a TDFL, about 2.8 mJ of pulse energy at 5 kHz was obtained by Mu *et al.*[16]. In 2011, 125 mJ at 100 Hz was reported through a master oscillator power amplifier (MOPA) system[19]. In 2013, Fonnum *et al.*[20] obtained the highest pulse energy thus far of 550 mJ at 1 Hz with a Ho:YLF crystal. In contrast, little work has been done on the high-energy results at a high pulse repetition frequency (PRF). In 2013, 11 mJ at 1 kHz was reported with a TDFL-pumped Ho:LLF MOPA system[21]. In 2013, 30 mJ at 1 kHz was reported in a Ho:YAG MOPA system with a Tm:YLF pump source by Yu *et al.*[22], and the pulse energy was enhanced to about 52 mJ in 2014[23]. Therefore, our main task is to develop a high-energy, high-PRF TDFL-pumped Ho:YAG laser system.

In this Letter, a high-power Ho:YAG oscillator pumped by a homemade TDFL is described, demonstrating its pulse characteristics at a high PRF. Its thermal characteristics were theoretically studied. In the CW regime, the maximum output power of 38 W at 2.09 μm was obtained, which is limited by the thermal lens effect. In the pulsed regime, with a relative high PRF of 1 kHz, the maximum pulse energy of 12.8 mJ at 2.09 μm was achieved when the corresponding CW output power was 17.6 W, but it was limited by the mirror coating damage.

A schematic diagram of the experimental setup is shown in Fig. 1. The 1.91 μm pump source is self-developed by a

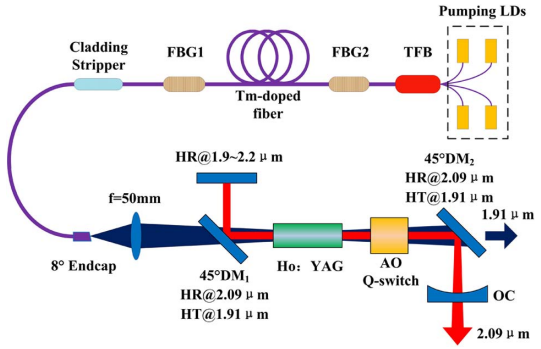

Fig. 1. Layout of the Ho:YAG laser end-pumped by a TDFL.

widespread all-fiber cladding-pumping technique. Four fiber-coupled 790 nm LDs (P2-070-0791-2-A-R01-S0043, nLight) were combined into one beamlet by using a 7×1 multimode combiner (MMC0701C3561, ITF Labs) to pump the gain fiber. The gain fiber was a 2 m-long double-clad Tm-doped fiber with a 25 μm circular core and a 400 μm octagonal inner cladding (LMA-TDF-25P/400-HE, Nufern) wrapped around a mandrel with a 28 cm diameter and cooled at a constant temperature of 283 K. A pair of fiber Bragg gratings (FBGs, ITF Labs) at the wavelength of 1907.7 nm (FBG_2 was highly reflective, $R_2 = 99.7\%$, and FBG_1 had low reflectance, $R_1 = 10\%$) were separately spliced to each end of the gain fiber to construct the laser cavity. Figure 2 shows the typical absorption spectrum of Ho:YAG and the transmission through a standard atmosphere[24,25]. Obviously, the pump wavelength of 1907.7 nm circumvents the water vapor absorption peak and is well centered within the Ho:YAG absorption peak. In addition, a homemade cladding stripper was used to remove the residual pump light and signal light that leaked into the cladding. The end facet was cut at an angle of 8° to reduce the feedback from the Fresnel reflection.

The 1.91 μm pump light was focused on a $1/e^2$ diameter of 560 μm inside the Ho:YAG crystal by a convex lens, $f = 50$ mm. A 0.6 at.%-doped Ho:YAG rod with a diameter of 4 mm and a length of 60 mm was used as the active medium. Both end faces of the crystal were anti-reflection coated at the pump and laser wavelengths. The crystal was wrapped in an indium foil layer and mounted in a copper heat sink that maintained a coolant water temperature of 283 K. In the experiment, we found that the TDFL was seriously influenced by the feedback from the reflected pump light, leading to a dramatic drop in the output power and the appearance of a new wavelength around 1980 nm. To prevent the pump source from being influenced by the feedback, the Ho:YAG crystal was placed in a Z-shaped cavity by using two 45° dichroic mirrors (DM_1 and DM_2, $R > 98\%$ at 2.09 μm, $T > 96\%$ at 1.91 μm). Additionally, a flat mirror ($R > 98\%$ at 1.9–2.2 μm) and a concave output mirror ($T = 50\%$ at 2.09 μm) with a curvature radius of 300 mm were employed. The physical length of the resonator was 220 mm. The Q-switch (I-QS027-4C10V5(BR)-U5-IS6, Gooch&-Housego), which is 50 mm long, has a maximum RF power of 100 W, while the PRF can be tuned continuously from 1 to 50 kHz.

Figure 3 presents the dependence of the output of the TDFL on the incident 790 nm LD pump power, which was measured with a power meter (OPHIR NOVA II: FL250 A-LP1-SH-V1). The maximum power of 81 W was achieved at the pump power of 200 W, corresponding to an optical-to-optical efficiency of 40.5% and a slope efficiency of 42.2%. The beam quality was measured as $M^2 = 1.56$ by using the knife-edge method. The inset of Fig. 3 shows the spectrum of the TDFL output laser with the central wavelength located at 1908 nm, measured with a spectral analyzer (SM301-EX, Spectral Products).

Figure 4 shows the output characteristics of the Ho:YAG laser during CW operation. Under the pump power of 81 W from the TDFL, the maximum output power of 38.5 W was obtained with an optical-to-optical efficiency of 47.5% and a slope efficiency of 51.9%. Meanwhile, the unabsorbed pump power was 11.1 W under the maximum incident pump power, so the actual conversion efficiency corresponding to the absorbed pump power reached 55.1%, and the slope efficiency corresponding to the absorbed pump power reached 64.3%. When the system was operating at the maximum output state, we found that the output power of 38.5 W became a little

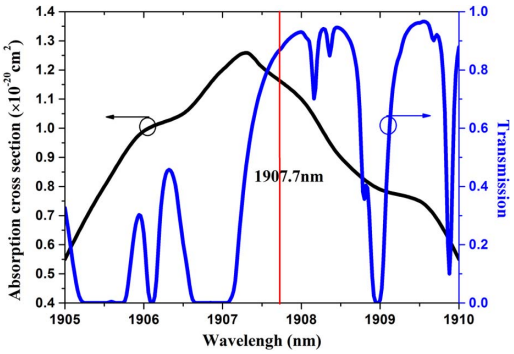

Fig. 2. Ho:YAG effective absorption cross section[24] (black curve) and transmission through a standard atmosphere[25] (blue curve).

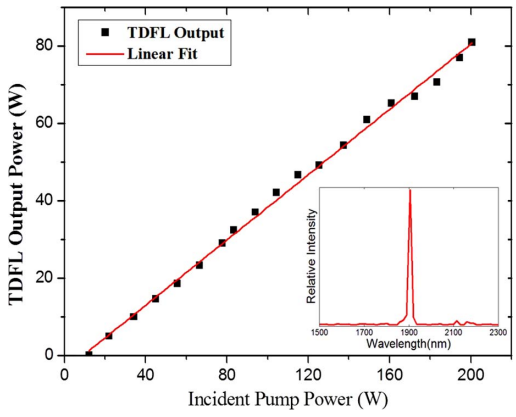

Fig. 3. Output power and spectrum of the TDFL pump source.

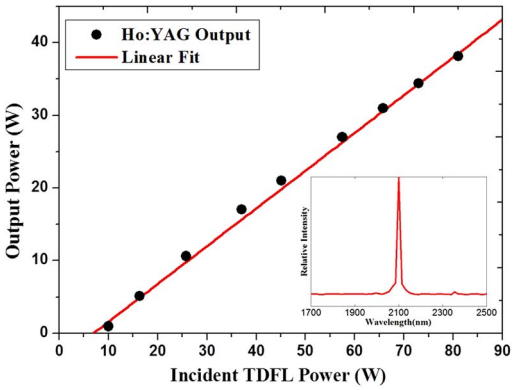

Fig. 4. Output power and spectrum of the Ho:YAG laser.

unstable, which may be mostly caused by the thermal lens effect. So it is worthwhile to investigate the thermal characteristics of a TDFL-pumped Ho:YAG laser, as discussed later. The inset of Fig. 4 shows the spectrum of the Ho:YAG output laser with the central wavelength located at 2100 nm. The beam quality measured in our experiment was $M^2 = 1.48$; it was measured using the knife-edge method. The lens ($f = 50$ mm) is located 70 mm away from the output coupler. The measured waist was 142 μm, so the TEM_{00} Gaussian beam waist radius was about 116 μm ($\omega_{TEM_{00}} = \omega/\sqrt{M^2}$).

At a PRF of 1 kHz, the dependence of the output power and the laser pulse width on the incident pump power was measured, as shown in Fig. 5. Although it was limited by the dichroic mirror's coating quality (damage threshold of about 835 MW/cm^2 at 2.09 μm), a maximum output energy of 12.8 mJ was obtained with a pump power of 37 W, corresponding to an optical-to-optical efficiency of 34.6% and a slope efficiency of 49%.

The minimum pulse width was less than 25 ns when the pump power was 37 W, corresponding to a peak power of approximately 514.5 kW, and the pulse width was shortened sharply as the incident pump power increased, as shown in Fig. 5. Furthermore, the dependence of the laser pulse width on the PRF was measured at the incident pump power of 37 W. The pulse width increased from 24.88 ns at 1 kHz to 81 ns at 50 kHz. Meanwhile, the

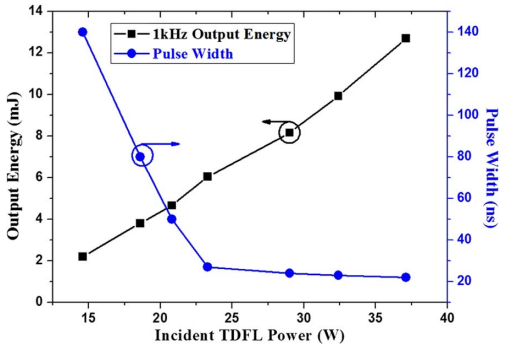

Fig. 5. Output power and pulse width of the Ho:YAG laser at a PRF of 1 kHz.

average power of the laser output increased from 12.8 to 16.2 W.

In the experiments above, the Ho:YAG laser's performance was found to heavily rely on the operation temperature as a quasi-three-level system[5]. Besides, the thermal lens effect would make the resonator unstable at high pump power levels. In the following, a basic thermal analysis is demonstrated.

Considering end-pumped Ho:YAG rods, the steady-state temperature distribution can be obtained by solving the heat transfer Poisson equation. With a cylindrically symmetrical laser crystal, the heat transfer equation is given by:

$$\frac{\partial^2 T(r,z)}{\partial r^2} + \frac{1}{r}\frac{\partial T(r,z)}{\partial r} = -\frac{Q(r,z)}{K_c}, \tag{1}$$

where $K_c = 14$ W/m/K is the thermal conductivity of Ho:YAG, and $Q(r,z)$ is the heat source as a Gaussian function.

Therefore, the heat source can be expressed as

$$Q(r,z) = \frac{2\alpha P_{\text{in}}\eta_h}{\pi\omega_p^2(z)} \exp\left(-\frac{2r^2}{\omega_p^2(z)} - \alpha z\right). \tag{2}$$

For conventional edge cooling, the rod-end thermal boundary conditions can be approximated as adiabatic. Thus, the solution of Eq. (1) for an isotropic crystal is derived using (similar to Ref. [26]):

$$\begin{cases} \Delta T(r,z) = T(r,z) - T(r_0,z) = \dfrac{\alpha P_{\text{in}}\eta_h \exp(-\alpha z)}{2\pi K_c} \\ \quad \times \left[1 - \frac{r^2}{\omega_p^2(z)} + \ln\left(\frac{r_0^2}{\omega_p^2(z)}\right) + \ln\left(\frac{r_0^2}{r^2}\right)\right] \\ \omega_p(z) = \omega_{p0}\sqrt{1 + \frac{\lambda_p|z-z_0|}{\pi n\omega_{p0}^2}} \end{cases}, \tag{3}$$

where $T(r_0,z) = 283$ K is the constant temperature at the surface of the laser crystal, $\omega_{p0} = 280$ μm is the pump beam waist radius, and $\omega_p(z)$ is the pump spot radius at a distance $(z - z_0)$ from the pump beam waist, $n = 1.82$ is the refractive index of the crystal, $\alpha = 0.33$ cm^{-1} is the absorption coefficient, $\eta_h = 1 - \lambda_p/\lambda_L = 0.09$ is the quantum defect, $r_0 = 2$ mm is the radius of the laser rod, $l_0 = 60$ mm is the length of the laser rod, and $P_{\text{in}} = 80$ W is the incident pump power.

The temperature distribution in the laser crystal is shown in Fig. 6, with the pump beam waist located within the crystal 30 mm away from the surface. It is shown that the peak temperature within the Ho:YAG rod is 402 K, and is located at the center of the pump incident face.

For a paraxial coherent beam propagating in the z-direction, the total optical path difference (OPD) for one round trip is given by[27]:

$$\text{OPD}(r) = 2\left[\frac{dn}{dT} + (n-1)(1+\nu)\alpha_T\right] \times \int_0^L \Delta T(r,z)\mathrm{d}z, \tag{4}$$

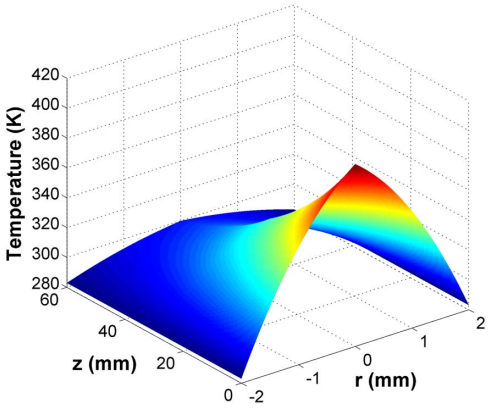

Fig. 6. Temperature distribution in an axial cross section of the Ho:YAG rod.

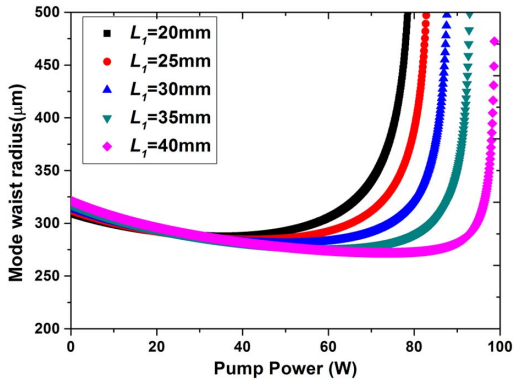

Fig. 8. Dependence of the beam size on the thermal focal length at different values of L_1.

where $dn/dT = 7.8 \times 10^{-6}$ K^{-1} is the temperature-dependent index change, and $(n-1)(1+\nu)\alpha_T$ is caused by temperature-dependent end-surface deformation, which relates to Poisson's ratio $\nu = 0.25$ and the thermal expansion coefficient $\alpha_T = 6.14 \times 10^{-6}$ K^{-1}.

Here, the OPDs caused by strain-induced birefringence and the shape distortion of end the face are neglected. So the corresponding OPD is given by:

$$\mathrm{OPD}(r) = \mathrm{OPD}_0 - \frac{r^2}{f_{\mathrm{th}}}, \tag{5}$$

where OPD_0 is the OPD at the center of the pump and f_{th} depicts the thermal focal length. For a laser crystal, f_{th} is determined by fitting the calculated space-resolved OPDs of Eqs. (3)–(5) over the extent of the beam radius inside the rod. According to the calculation, the thermal focal length decreases along with the growth of pump power, from $f_{\mathrm{th}} = 1214$ mm when $P_{\mathrm{in}} = 10$ W to $f_{\mathrm{th}} = 153$ mm when $P_{\mathrm{in}} = 80$ W.

The beam light propagates as illustrated in Fig. 7. The thermal lens in a laser resonator can be assumed to be an ideal thin lens. In our experiment, a compact system in package is necessary, and the shortest cavity length L is about 220 mm, while L_1 is in the range of 15–45 mm.

The radius of the TEM_{00} mode on the laser crystal with different values of L_1 and pump powers can be calculated[28] as shown in Fig. 8. It can be seen that inflection points of all the curves will emerge when the pump power is high enough, but the one with a larger value of L_1 appears at higher pump power, suggesting that the signal spot can remain in good overlap with the pump spot over a wider range of pump powers. Meanwhile, the cavity becomes unstable when L_1 is less than 25 mm and the pump power is higher than 80 W, which is detrimental to the power scaling. Thus, in our experiment, the value of $L_1 = 40$ mm was chosen, and the radius of the TEM_{00} mode on the laser crystal is around 300 μm when the pump power ranges from 0 to 90 W, which is well matched with our pump light.

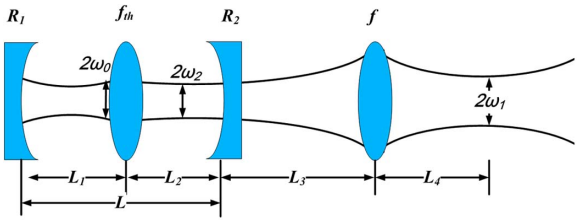

Fig. 7. Transformation of the output beam for a stable resonator containing a thermal lens f_{th}.

A useful method to assess the accuracy of the theoretical model is based on the use of a supplementary focus lens with the known pump power and the position of the test beam waist. According to the above measurement of the beam quality, a lens ($f = 50$ mm) is used at a distance of 70 mm away from the output mirror. When pump power is 80 W, the calculated thermal focal length was about 153 mm, so we can work out that the theoretical TEM_{00} mode beam waist through the lens ($f = 50$ mm) is about 143 μm. In our experiment, the TEM_{00} Gaussian beam waist radius was measured as 116 μm, so the calculated Gaussian beam waist radius is a little larger than the measured one. This result may be caused by the assumption that the thermal lens in a thermally loaded material is an ideal thin lens, while it is in fact a thick lens.

In conclusion, a maximum CW power of 38 W with a slope efficiency of 51.9% is achieved using a Z-shaped Ho:YAG oscillator resonantly pumped by a homemade TDFL. The beam quality factor of $M^2 \approx 1.48$ is measured using the knife-edge method. In the Q-switching regime, a single pulse energy of 12.8 mJ is obtained with a PRF of 1 kHz and a pulse width of 25 ns. A thermal analytical model for a TDFL-pumped Ho:YAG oscillator is also performed. In this model, the radius of the TEM_{00} mode on the laser crystal under different pump powers is analyzed, and is confirmed to be in agreement with the experimental results. The output pulse energy can be improved by expanding the pump spot and optimizing the cavity parameters.

This work was supported by the National Natural Science Foundation of China (No. 61275146), the Research

Fund for the Doctoral Program of Higher Education of China (No. 20120002110066), and the Special Program of Co-Construction with the Beijing Municipal Government of China (No. 20121000302).

References

1. E. Lippert, G. Rustad, G. Arisholm, and K. Stenersen, Opt. Express **16**, 13878 (2008).
2. R. J. De Young and N. P. Barnes, Appl. Opt. **49**, 562 (2010).
3. P. A. Budni, L. A. Pomeranz, M. L. Lemons, C. A. Miller, J. R. Mosto, and E. P. Chicklis, J. Opt. Soc. Am. B **17**, 723 (2000).
4. S. D. Jackson, A. Sabella, and D. G. Lancaster, IEEE J. Sel. Top. Quant. **13**, 567 (2007).
5. M. Eichhorn, Appl. Phys. B-Lasers O **93**, 269 (2008).
6. L. Han, B. Yao, X. Duan, S. Li, T. Dai, Y. Ju, and Y. Wang, Chin. Opt. Lett. **12**, 081401 (2014).
7. J. W. Kim, J. I. Mackenzie, D. Parisi, S. Veronesi, M. Tonelli, and W. A. Clarkson, Opt. Lett. **35**, 420 (2010).
8. S. Lamrini, P. Koopmann, K. Scholle, and P. Fuhrberg, Opt. Lett. **38**, 1948 (2013).
9. W. Wang, F. Tang, X. Yuan, C. Ma, W. Guo, and Y. Cao, Chin. Opt. Lett. **13**, 051404 (2015).
10. X. Yang, H. Huang, D. Shen, H. Zhu, and D. Tang, Chin. Opt. Lett. **12**, 121405 (2014).
11. G. A. Newburgh, A. Word-Daniels, A. Michael, L. D. Merkle, A. Ikesue, and M. Dubinskii, Opt. Express **19**, 3604 (2011).
12. V. Jambunathan, X. Mateos, M. C. Pujol, J. J. Carvajal, F. Díaz, M. Aguiló, U. Griebner, and V. Petrov, Opt. Express **19**, 25279 (2011).
13. L. J. Li, B. Q. Yao, and Y. Z. Wang, Laser Phys. **19**, 1223 (2009).
14. B. Q. Yao, G. Li, P. B. Meng, G. L. Zhu, Y. L. Ju, and Y. Z. Wang, Laser Phys. Lett. **7**, 857 (2010).
15. G. Rustad and K. Stenersen, IEEE J. Quantum Electron. **32**, 1645 (1996).
16. X. D. Mu, H. Meissner, and H. C. Lee, Proc. SPIE **7686**, 76860T (2010).
17. Y. J. Shen, B. Q. Yao, X. M. Duan, T. Y. Dai, Y. L. Ju, and Y. Z. Wang, in *Conference Lasers and Electro-Optics* (2013), CTu3D.3.
18. S. Lamrini, P. Koopmann, M. Schafer, K. Scholle, and P. Fuhrberg, Appl. Phys. B-Lasers O **106**, 315 (2012).
19. K. Schmidt, C. Reiter, H. Voss, F. Maßmann, and M. Ostermeyer, in *Conference Lasers and Electro-Optics* (2011) CA3_4.
20. H. Fonnum, E. Lippert, and M. W. Haakestad, Opt. Lett. **38**, 1884 (2013).
21. A. Dergachev, Proc. SPIE **8599**, 85990B (2013).
22. K. K. Yu, X. M. Duan, D. X. Zhang, B. Q. Yao, and Y. J. Shen, Laser Phys. **23** (2013).
23. C. P. Qian, B. Q. Yao, X. M. Duan, Y. L. Ju, K. K. Yu, and Y. Z. Wang, Chin. Phys. Lett. **31** (2014).
24. D. C. Brown, V. Envid, and J. Zembek, Appl. Opt. **51**, 8147 (2012).
25. Gemini Observatory, http://www.gemini.edu (accessed April 16, 2010).
26. M. E. Innocenzi, H. T. Yura, C. L. Fincher, and R. A. Fields, Appl. Phys. Lett. **56**, 1831 (1990).
27. Y. F. Chen, J. Opt. Soc. Am. B **17**, 1835 (2000).
28. I. N. Duling, R. P. Moeller, W. K. Burns, C. A. Villarruel, L. Goldberg, E. Snitzer, and H. Po, IEEE J. Quantum Electron. **27**, 995 (1991).